MOLEKUL
eISSN: 2503-0310

Articles
https://doi.org/10.20884/1.jm.2024.19.3.8521

Activated Charcoal Magnetic Composite from Jengkol Peels as An Efficient Adsorbent for Aquatic Antibiotic Removal: An in Vitro Study

Gatut Ari Wardani[1]*, Mia Nurhidah[1], Winda Trisna Wulandari[1], Estin Nofiyanti[2], Ricky Andi Syahputra[3], Indra Indra[1]

[1]Program Study of Pharmacy, Universitas Bakti Tunas Husada, Indonesia
[2]Program Study of Environmental Engineering, Universitas Muhammadiyah Tasikmalaya, Tasikmalaya, Indonesia
[3]Program Study of Chemistry, Universitas Negeri Medan, Indonesia

*Correspondence: E-mail: gatutariwardani@universitas-bth.ac.id

Received June 09, 2023; **Accepted** August 19, 2024; **Available online** November 20, 2024

ABSTRACT. Antibiotic resistance has become a global issue that is quite worrying because it can threaten the survival of living things, especially humans. This resistance can occur due to the inappropriate use of antibiotics by the community. This study aims to determine the ability of activated charcoal magnetic composites (ACMC) to adsorb tetracycline hydrochloride compounds. Samples were obtained from jengkol peel waste which was charred and activated using acid and the addition of magnetic properties. The more $PbFe_2O_4$ added to activated charcoal, the greater the magnetic properties, surface area, pore-volume, and pore radius. The results showed that a type of IV adsorption isotherm which is a characteristic of mesoporous materials with a pore size of 2.0892 nm. The addition of magnetic properties to activated charcoal increase 29.33% the amount of tetracycline that is adsorbed by the adsorbent with optimal absorption in alkaline conditions. The adsorption process followed the adsorption kinetics of Ho and the Freundlich adsorption isotherm with an adsorption capacity of 76.3359 mg/g. ACMC material can potentially be one of the adsorbents that can reduce contamination of tetracycline hydrochloride antibiotics in the aquatic environment so that antimicrobial resistance can be minimized.

Keyword: acidity, agricultural waste, carbonization, functional Group, VSM analysis

INTRODUCTION

Antibiotics are very important to fight infection due to bacteria, widely used in medicine, animal husbandry, and aquaculture to kill or inhibit the growth of bacteria (Wang et al., 2020). Humans or animals cannot directly metabolize antibiotics, and most are excreted in the form of the original drug or parent compound into the environment (Singh et al., 2019). One of the antibiotic compounds used is a type of Tetracycline. About 70% of Tetracycline Hydrochloride taken by mouth is excreted in the urine (Daghrir & Drogui, 2013; Martins et al., 2015).

In nature, most of the Tetracycline Hydrochloride effluent is released into surface water, underground water, into the soil environment in its original form through soil infiltration (Akhtar et al., 2016). This is due to the widespread use of tetracycline antibiotics, especially in the medical and agricultural sectors (Akhtar et al., 2016; Daghrir & Drogui, 2013). Tetracycline Hydrochloride waste in the aquatic environment can cause bacterial resistance, cause ecological damage and threaten human health through bioaccumulation in the food chain (Guo et al., 2017). Tetracycline Hydrochloride is classified as a potential pollutant in many countries because it causes serious damage to the environment (Conde-Cid et al., 2018). The natural low removal efficiency of Tetracycline Hydrochloride is an urgent need to develop an effective and economical remediation technology to control antibiotics in the environment. Adsorption is the most commonly used technique in wastewater treatment (Zhang et al., 2017).

Porous materials are widely used as adsorbents to absorb pollutants in the aquatic environment. This ability is possessed because of the properties of porous materials, including (i) homogeneous pore size, (ii) high surface area, and (iii) controlled pore structure and surface properties (Sun et al., 2016). One of the porous materials that are often used for adsorption is activated charcoal. However, the utilization of jengkol peel which is modified into Activated charcoal magnetic composites as an antibiotic adsorbent has not been widely studied.

Jengkol peel has a total carbon element of 44.02% (Gusnidar et al., 2011), which is believed to be the most important element that has the potential to be used as activated charcoal as an adsorbent. When jengkol peel is made into activated carbon, the carbon

content increases to 92.87% (Azima et al., 2017). Activated carbon or activated charcoal is a suitable adsorbent to remove organic compounds in water (Bhatnagar et al., 2013; Nielsen et al., 2014; Bakas et al., 2014). Modified activated charcoal can increase its ability as an adsorbent to absorb organic compounds. This can happen because the modification of activated charcoal, such as Fe^{3+} ions, can increase the surface area, total pore volume, micropore volume, and mesopore volume (Liu et al., 2017). Modified activated charcoal is then referred to as Activated Charcoal Magnetic Composite (ACMC)

The combination of adsorbent with magnetic particles produces a new composite material with dual properties: adsorption and magnetic characteristics. This magnetic property is utilized to separate composite particles from water using a simple magnetic bar, making the process easier, simpler, faster, and more efficient in retrieving the adsorbent from the waste liquid. Additionally, the use of magnetic composites in antibiotic adsorption offers several advantages over conventional adsorbents. (Sivashankar et al., 2014). magnetic materials such as Fe_3O_4 in carbon nanotube (CNT) composites exhibit high adsorption capacity and can be easily separated from aqueous media using an external magnetic field (Liu et al., 2019). High-porosity magnetic composites, such as Fe_3O_4@HKUST-1, possess superior capabilities in rapid desorption through magnetic induction heating, thereby enhancing the efficiency of the adsorbent regeneration process. Moreover, the thermal and chemical stability of magnetic composites allows for their reuse in multiple adsorption cycles without significant loss of performance, making them more economical and sustainable. In the context of water treatment, this technology provides a practical solution for removing contaminants like antibiotics from water sources, both at laboratory and industrial scales (Bellusci et al., 2024). Therefore, the utilization of magnetic composites in this study is expected to contribute significantly to the development of more effective and efficient water treatment methods

EXPERIMENTAL SECTION

Preparation of Magnetic Composite

To prepare the magnetic composite, a specific amount of activated charcoal derived from jengkol peels was added to 200 mL of a solution containing lead (II) nitrate and iron (II) chloride at room temperature. The amount of activated charcoal was carefully adjusted to achieve mass ratios of $PbFe_2O_4$ to activated charcoal at 1:1 (referred to as ACMC 11), 3:1 (ACMC 31), and 1:3 (ACMC 13). Sodium hydroxide solution was then added dropwise to the mixture while continuously stirring until the pH reached 11. The suspension was then heated at 100 °C for 4 hours using a water bath to ensure thorough interaction and composite formation. After heating, the suspension was allowed to cool to room temperature. The formed magnetic composite was then carefully washed with demineralized water (aqua DM) until the wash water reached a neutral pH, indicating the removal of residual reagents. The clean composite was separated from the water using a simple magnet, exploiting its magnetic properties. Finally, the separated composite was dried in an oven at 110 °C until a constant weight was achieved, ensuring complete moisture removal and preparation of the composite for further testing. The magnetic composite was characterized using Fourier-transform infrared spectroscopy (FTIR) to identify functional groups, X-ray diffraction (XRD) to analyze crystal structure, Scanning Electron Microscopy (SEM) to observe surface morphology, a Surface Area Analyzer (SAA) to measure specific surface area and pore volume, and Vibrating Sample Magnetometry (VSM) to study and application of magnetic materials.

Adsorption Isotherm Study

The adsorption isotherm study was conducted to understand the relationship between the amount of antibiotic adsorbed onto the adsorbent surface and the antibiotic concentration in the solution at equilibrium. For this analysis, solutions of tetracycline hydrochloride with various concentrations (25, 50, 75, 100, and 125 ppm) were prepared and added to 50 mL of solution containing a fixed amount of the magnetic activated carbon adsorbent. Each solution was stirred using a magnetic stirrer at 200 rpm at room temperature until equilibrium was reached. After the adsorption process, the solutions were filtered, and the remaining antibiotic concentration in the solution was analyzed using UV–Vis spectrophotometry. The data obtained were used to determine the most suitable isotherm model, such as Langmuir or Freundlich isotherms.

Adsorption Kinetics Study

The adsorption kinetics study was conducted to determine the rate and mechanism of antibiotic adsorption onto the adsorbent surface. For this analysis, a fixed concentration (20 mg/L) of tetracycline hydrochloride solution was prepared, and a specific amount of magnetic activated carbon adsorbent was added to 50 mL of the solution. Each solution was stirred at 200 rpm at room temperature, and samples were taken at different time intervals (30, 60, 90, 120, and 150 minutes). The collected samples were filtered, and the remaining antibiotic concentration was analyzed using UV–Vis spectrophotometry. The adsorption kinetics data were analyzed using first-order and second-order kinetics models to determine the kinetic parameters and understand the underlying adsorption mechanism.

In Vitro Adsorption Experiment

For the in vitro adsorption experiments, a standard solution of tetracycline hydrochloride (20 mL) was prepared at the optimum concentration determined from preliminary studies. Varying masses of the

magnetic activated carbon composite (5, 10, 15, 20, and 25 mg) were added to this solution. The resulting mixture was stirred at a constant speed of 200 rpm for 30 minutes at room temperature to allow sufficient interaction between the antibiotic and the adsorbent. After the adsorption process was completed, a magnet was brought close to the side of the beaker to collect the magnetic activated carbon, gathering it against the wall of the beaker that was in contact with the magnet, thus separating the adsorbent from the solution. The collected samples were filtered, and the remaining antibiotic concentration was analyzed using UV-Vis spectrophotometry.

RESULTS AND DISCUSSION

The quality of the activated charcoal produced was determined by testing the water content, ash content, the absorption capacity of methylene blue, and the absorption of iodine (**Table 1**). Parameters of activated charcoal compared with Indonesian National Standard number of 06-3730-1995. All characteristic results meet the Indonesian Nastional Standard regarding technical activated charcoal.

Fourier Transform Infra Red (FTIR)

The results of the prediction of the adsorbent functional group using FTIR (**Table 2**), jengkol peel powder informs the presence of an absorption band at a wavenumber of 3397 cm^{-1}, vibrations appear in the O-H group. This vibration is supported at the absorption of 1207 cm^{-1} which is a C-O vibration. At the wave number 1518 cm^{-1}, there are C = C vibrations from the aromatic ring; at wavenumbers, 2929 cm^{-1} and 1447 cm^{-1} are the vibrations from the C-H group. In jengkol peel charcoal, absorption appears at a wavenumber of 3408 cm^{-1}, vibrations in the OH group show that after the carbonization process, the intensity of the OH vibration decreases, the wavenumber is 1595 cm^{-1} vibrations from the C=C group, the CO group appears at a wavelength of 1252 cm^{-1}. On activated charcoal, absorption appears at a wavenumber of 3424 cm^{-1} vibrations on the OH group, an indication of hydrogen bonding between the hydroxy group and water absorbed on the surface of the activated charcoal, wave number 1579 cm^{-1} vibrations from the C=C group, the CO group appears at a wavelength of 1176 cm^{-1} wave originating from the vibrations of CO in the acid, alcohol, phenol, or ether groups.

The FTIR analysis was carried out on the magnetic composite of the adsorbed activated charcoal. The wavenumber at 600-400 cm^{-1} indicated the presence of vibrations from the Fe-O absorption, namely with a wavenumber of 543 cm^{-1} at ACMC 11 and 407 cm^{-1} at ACMC 11 and Pb-O bonds appeared at wavenumbers 681 cm^{-1} at ACMC 11 and 680 cm^{-1} at ACMC 31 which were not found in the activated charcoal spectra. At ACMC 13, there is no vibration from Fe-O absorption and Pb-O absorption; this can be caused by the lack of intensity of Fe-O and Pb-O bonds from magnetite and activated charcoal.

Table 1. Characteristics results of jengkol peel activated charcoal

Parameters	Indonesian National Standard	Research result
Water content	Max 15%	1.58 %
The absorption of iodine	Min 750 mg/g	995.0579 mg/g
The absorption of methylene blue	Min 120 mg/g	138.2009 mg/g
Ash content	Max 10%	1.45%

Table 2. Adsorbent functional groups based on FTIR characterization.

Func-tional Groups	compou nd type	Wavenumber (cm^{-1})	Jengkol peel (cm^{-1})	Char-coal (cm^{-1})	Activa-ted charcoal (cm^{-1})	ACMC 11 (cm^{-1})	ACMC 13 (cm^{-1})	ACMC 31 (cm^{-1})
O – H	Alcohol, phenol	3200-3600	3397	3408	3424	3427	3426	3406
C – H	Alkane	2850-2970 1340 -1470	2929 1447	-	-	- 1400	- 1391	- 1399
C ≡ C	Alkyne	2100-2260	-	-	-	-	-	-
C = C	aromatic ring	1500-1600	1518	1595	1579	-	1575	-
C = C	Alkyne	1600 - 1680	1615	-	-	1602		1612
C – O	Alcohol, Ether, carboxyli c acid, Esther	1050-1300	1207	1252	1176	-	-	-
Fe – O		600-400	-	-	-	543	-	407
Pb – O			-	-	-	681	-	680

Thus, jengkol skin can be clearly distinguished by its spectra from other materials (charcoal, activated charcoal, ACMC 11, ACMC 31, and ACMC 13). However, the spectra of charcoal, activated charcoal, ACMC 11, ACMC 31, and ACMC 13 could not be clearly distinguished so the FTIR analysis was not able to provide more information on the five samples. This can be determined by using principal component analysis (PCA) and cluster analysis (CA).

The Results of The Identification of the FTIR Spectra using PCA and CA

When viewed from the absorption in the FTIR (**Table 2**), it is not possible to clearly distinguish the spectral pattern between charcoal, activated charcoal, and modified charcoal. PCA is used to group similar data by reducing multivariate data in which there is a correlation between variables. All samples (**Table 2**) were analyzed using the PCA method except the jengkol peel (**Figure 1**).

The five samples have different groups. PC-1 can distinguish 48% with charcoal, ACMC 11, ACMC 13, and ACMC 31 are located in the same group, while activated charcoal is located in different groups. PC-2 differentiated the data by 34% by placing charcoal, ACMC 13, and ACMC 11 in the same group, while activated charcoal was in one group with ACMC 31. However, overall ACMC 31 was very different from the other samples, while activated charcoal was not. can be separated by PC-2 because it is close to point 0 on PC-2.

The position of activated charcoal and ACMC 11 on PCA did not give good separation results on PC-2. Therefore, a cluster analysis was carried out (**Figure 2**) to divide the sample into a group so that similar samples would be in the same group. The five samples were successfully grouped by type. The ACMC 31 material has a very big difference compared to the other four samples. ACMC 11 and ACMC 13 materials can be grouped into the same group because they do not have much difference. Likewise, charcoal and activated charcoal are grouped in the same group.

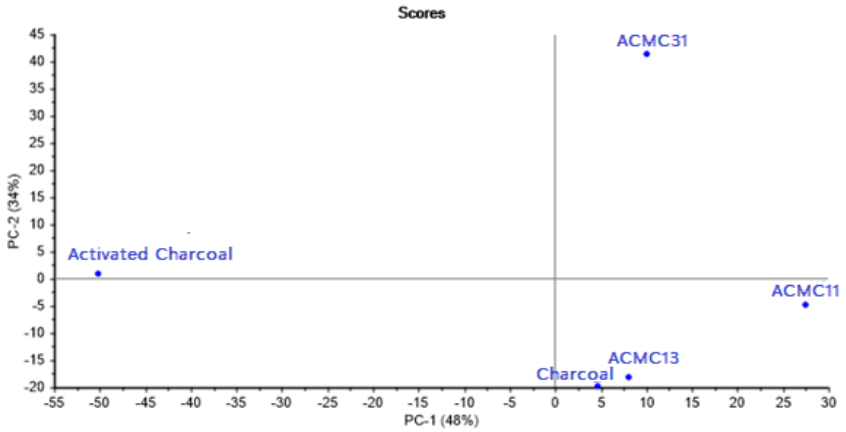

Figure 1. Principal component analysis (PCA) of adsorbent material based on FTIR spectra

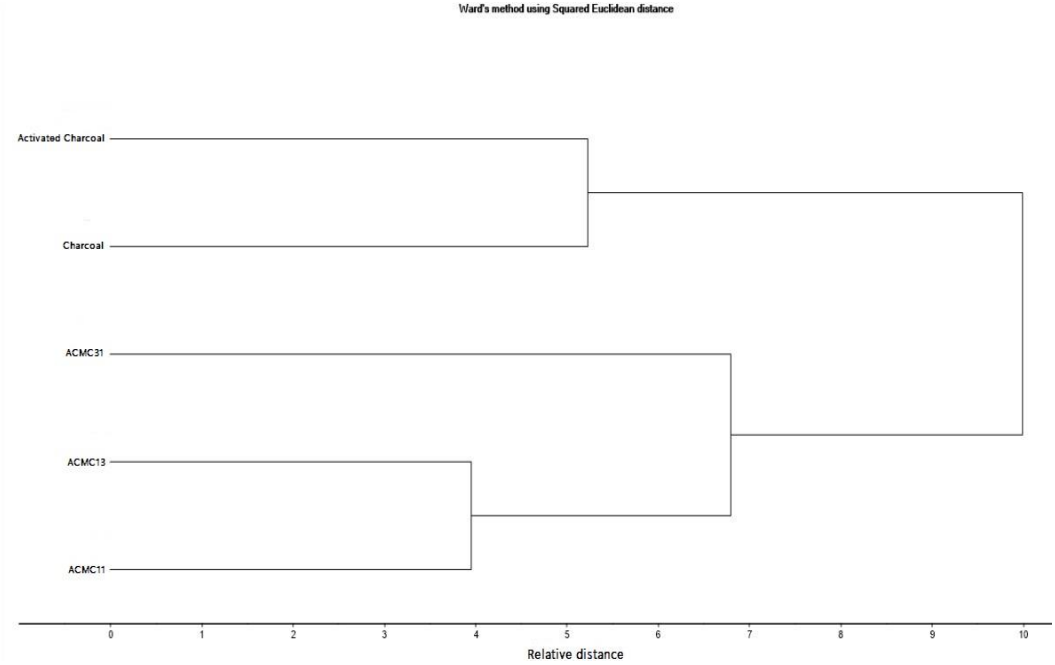

Figure 2. Cluster analysis (CA) of adsorbent material based on FTIR spectra

Adsorbent Morphology Based on SEM and XRD Characterization

The SEM characterization of the adsorbent aims to determine the surface morphology. The surface morphology of charcoal before and after activation was identified using SEM with an object magnification of 2500 times (**Figure 3**). Morphological analysis of the surface shape was carried out by Scanning Electron Microscopy (SEM), which showed the adsorbent surface shaped like a hollow sponge with many pores on the surface of the charcoal before and after activation. $PbFe_2O_4$ particles with various diameters were distributed on the activated charcoal surface. Although many small aggregates of lead ferrite covered the activated charcoal surface, the porous structure of activated charcoal could still be observed, which maintained the adsorption power of activated charcoal (Shao et al., 2012). X-ray diffraction analysis was carried out using an XRD device with a wavelength of 1.54 nm using radiation from a Cu target tube, and the observation area was between 5.00° – 79.99° (**Figure 4**).

The crystallinity data for the charcoal sample before activation, there were 4 peaks in the 2θ region, namely 14.93°, 24.46°, 28.37°, and 40.48°. There are 2 main peaks in charcoal after activation, which are in the 2θ region with values of 26.66° and 40.39°, which are different from the value of 2θ in the charcoal diffractogram before activation. The appearance of peaks 26.66° and 40.38° in the charcoal can be possible due to impurities in the charcoal. Impurities contained in the charcoal can be removed by the activation process into activated charcoal using 15% phosphoric acid. This is indicated by the loss of the two peaks in the activated charcoal sample. The XRD pattern of activated charcoal shows a broad weak diffraction peak between 20° and 30°, which indicates that the activated charcoal is amorphous (Wang et al., 2013). There is a shift in the value of 2θ to a smaller one in the charcoal after activation; this indicates that the pores of the activated charcoal are wider than the charcoal before activation due to the activation process (Shi et al., 2019).

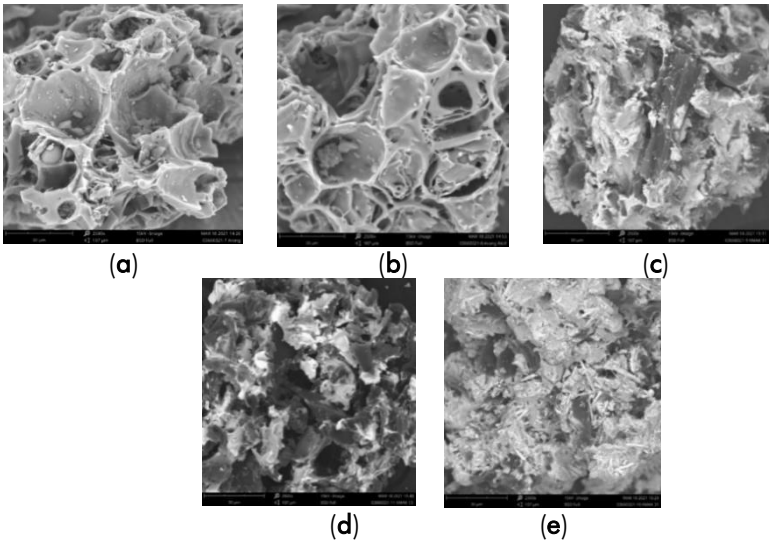

Figure 3. SEM results at 2500x magnification (**a**) Charcoal before activation (**b**) Charcoal after activation (**c**) ACMC 11 (**d**) ACMC 13 (**e**) ACMC 31

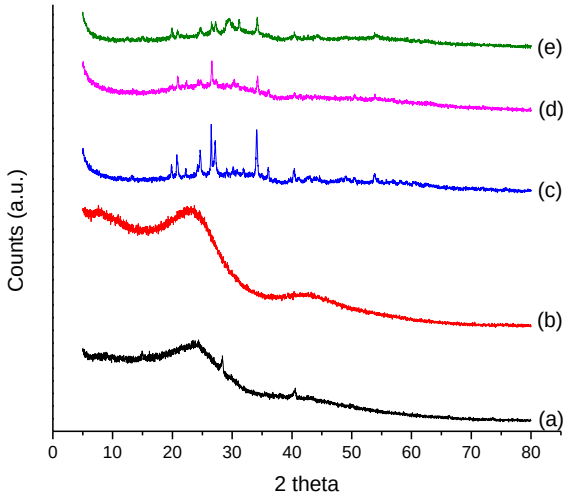

Figure 4. XRD Results of (**a**) Charcoal, (**b**) Activated Charcoal, (**c**) ACMC 11, (**d**) ACMC 13, and (**e**) ACMC 31

Surface Area Analyzer (SAA)

The magnetic composite diffraction pattern of activated charcoal in **Figure 3** matches the amcsd 0013508 code database of γ-Fe_2O_3 with the result that the value of 2θ confirming the presence of γ-Fe_2O_3 in the pores of the activated charcoal. Iron metal is in the form of oxide; the addition of Fe^{2+} tends to increase the formation of γ-Fe_2O_3.

PbO compounds are formed due to the presence of excess Pb^{2+} ions to form Pb in the form of oxides with the formation of peaks at $PbFe_2O_4$/Activated Carbon 1:1 31.89°, 48.23°; $PbFe_2O_4$/Activated Carbon 3:1 31.17° have the same value of 2θ (Lin et al., 2020). The $PbFe_2O_4$/Activated Charcoal composite has similar peaks with Fe_2O_3/Activated Charcoal and PbO/Activated Charcoal used as a comparison.

Various treatments given to magnetically activated charcoal adsorbents can produce different characteristics (surface area, pore-volume, and pore spacing) of the adsorbent. The surface area of the adsorbent can be determined using the Brunauer-Emmett-Teller (BET) method. In contrast, the pore volume and pore spacing are determined using the Barrett-Joyner-Halenda (BJH) method. The activation process of charcoal material (**Table 3**) can increase the surface area from 11.684 m^2/gram to 73.089 m^2/gram (525.55 %).

In addition to the surface area, the pore volume also increased by 157.14% with the smaller pore size. The smaller pore size and the increased surface area and pore volume indicate increasing pores during the activation process. To increase the absorption of the adsorbent, it is necessary to modify it by providing magnetic properties so that it becomes a magnetic-activated charcoal composite further. The addition of magnetic properties using a ratio of $PbFe_2O_4$/activated charcoal 3:1 (ACMC 31) is known to have the largest surface area, pore-volume, and pore radius. Thus, the greater the ratio of $PbFe_2O_4$/activated charcoal, the surface area of the adsorbent will increase, as well as the pore volume and pore radius. The pore size of ACMC 31 of 20.892 Å or 2.0892 nm belongs to the mesopore composite (2 – 50 nm). At the same time, the other variations (charcoal, activated charcoal, ACMC 11, and ACMC 13) are included in the micropore composite, which has a pore size of less than 2 nm (Pérez-Ramírez et al., 2008).

Mesopore carbon has its advantages, including regular pore structure, narrow pore distribution, large and specific surface area, and excellent chemical and physical stability (Nejad et al., 2013). The large pore size supports the ability to absorb tetracycline hydrochloride compounds well. The adsorption of tetracycline hydrochloride by ACMC 31 indicated a type IV adsorption (**Figure 5**).

Table 3. The results of the characterization of the adsorbent using the BET and BJH methods

Sample	BET Method	BJH Method	
	Surface Area (m^2/gram)	Pore volume (cc/gram)	Pore radius (Å)
Charcoal	11.684	0.014	16.921
Activated charcoal	73.089	0.036	15.571
ACMC 11	60.895	0.092	19.442
ACMC 13	48.988	0.068	15.538
ACMC 31	75.242	0.130	20.892

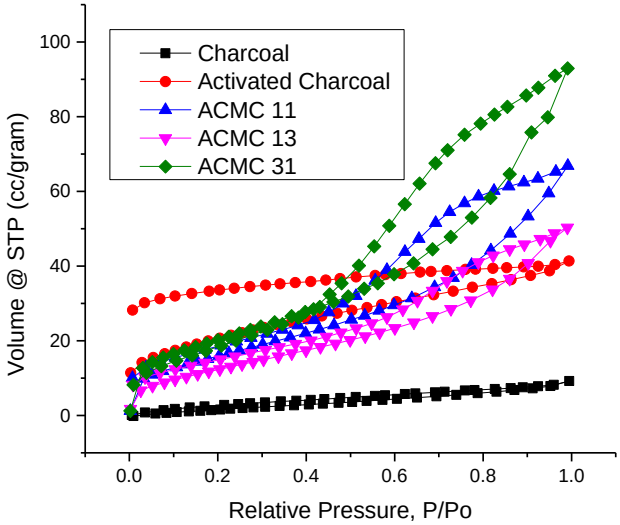

Figure 5. Nitrogen adsorption and desorption isotherms of (**a**) charcoal, (**b**) activated charcoal, (**c**) ACMC 11, (**d**) ACMC 13, and (**e**) ACMC 31

The hysteresis loop in ACMC 31 was more pronounced than in the other samples. This indicates that the material is mesoporous (Farzin Nejad et al., 2013). Type IV adsorption shows the dominant pore shape in the form of wedge and parallel plates (Ding et al., 2021).

Vibrating Sample Magnetometer (VSM)

The magnetic properties of the activated charcoal magnetic composite adsorbent were compared to charcoal before activation and charcoal after activation, so measurements were made using a VSM. The data obtained from this test is in the form of a hysteresis curve. The results of the VSM analysis (**Figure 6**) can be seen that the activated charcoal magnetic composite has a small magnetizing property. For activated charcoal magnetic composites with a ratio of 1:1 and 3:1, a linear curve is formed, inclined towards paramagnetic properties, namely objects that can be weakly attracted by magnets. If we apply an external magnetic field, the direction of the magnetic moment tends to line up with the external magnetic field, thus exhibiting a paramagnetic effect.

According to the research of Smitha et al., 2008, the saturation magnetization of $PbFe_2O_4$ is 0.52 emu/g. The saturation magnetization decreases after the magnet is composited with activated charcoal (**Figure 7**). This is because there is a non-magnetic fraction, namely activated charcoal, in the composite. The higher the non-magnetic fraction in the composite, the more saturation magnetization also decreases. The saturation magnetization decreases after the magnetization is composited with activated charcoal. This is due to the presence of non-magnetic fractions such as activated carbon in the composite. The characterization results with VSM showed that the sample with the most Fe^{2+} administration produced a high saturation magnetization value. Thus, it can be concluded that this sample has the best magnetic properties.

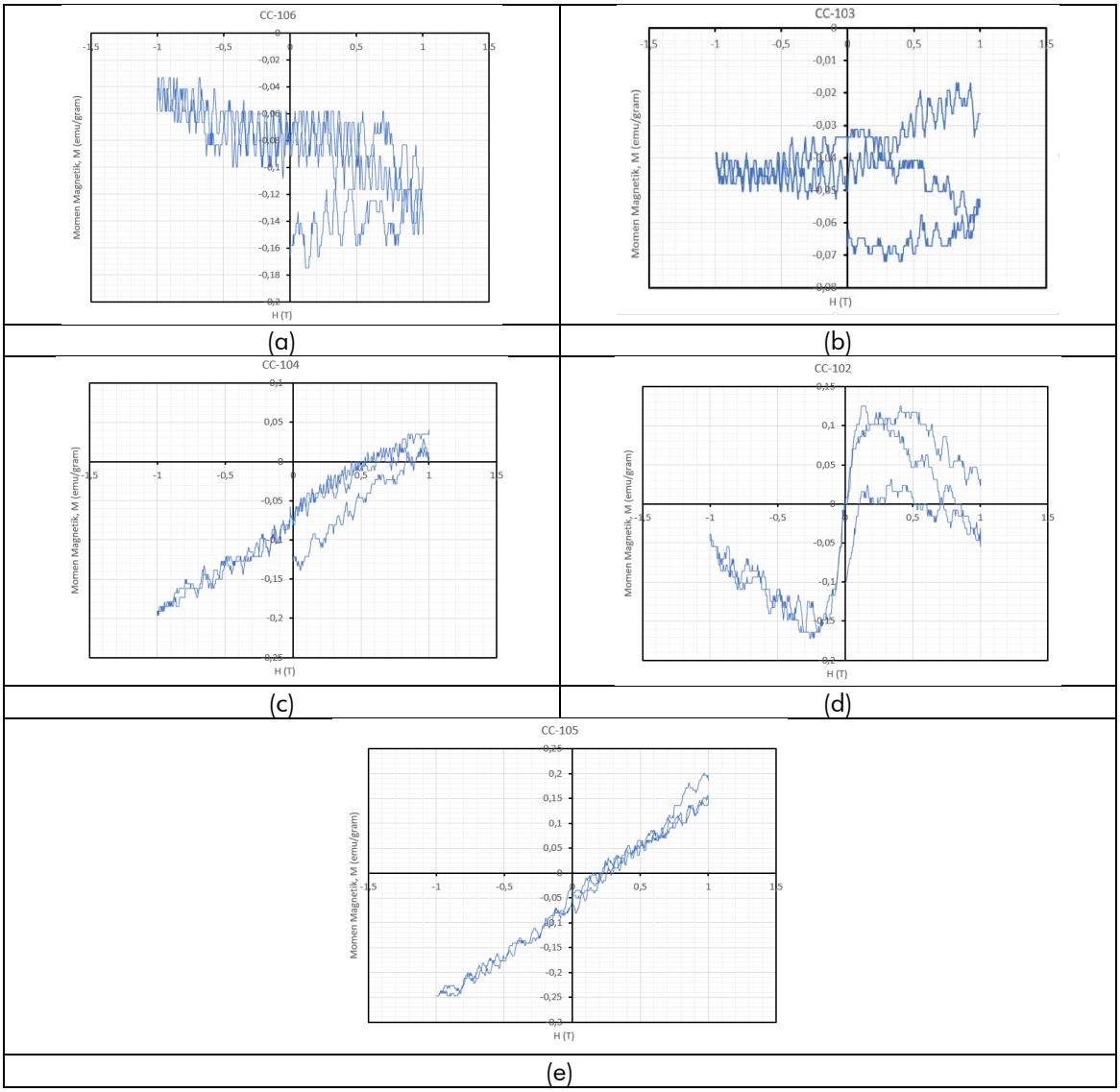

Figure 6. The results of the analysis of the magnetic properties of the adsorbent (**a**) Charcoal before activation (**b**) Charcoal after activation (**c**) ACMC 11 (d) ACMC 13 (e) ACMC 31

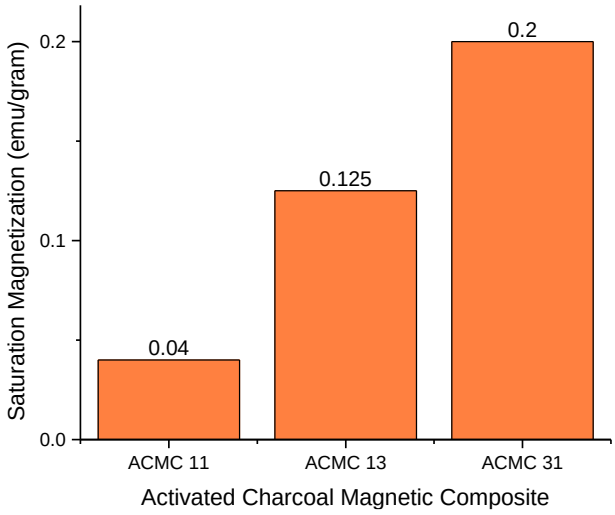

Figure 7. Magnetization value of activated charcoal magnetic composite

The adsorbed concentration of tetracycline hydrochloride increases with the increase in the mass of the adsorbent (**Figure 8**). The adsorbent mass of 15 mg was the best because there had been a balance between the tetracycline hydrochloride absorbed by the adsorbent and the amount of remaining in the solution so that the adsorbent had maximally bound the tetracycline hydrochloride. Meanwhile, the mass of more than 15 mg decreased the adsorption of tetracycline hydrochloride. This is due to overlapping events during the adsorption process due to the density of the adsorbent particles. This density causes the surface area of the adsorbent to be smaller so that the active site of the adsorbent is reduced. In this study, the best adsorbent mass of activated charcoal and magnetic composites of activated charcoal 3:1 was 15 mg with a concentration of tetracycline hydrochloride adsorbed from activated charcoal of 1.3253 ppm and of magnetic composites of activated charcoal 3:1, which were 7.7769 ppm.

In this study, the magnetic composite of activated charcoal 3:1 absorbs more tetracycline hydrochloride than activated charcoal. This is due to the adsorption mechanism that occurs between the hydroxyl group present in tetracycline hydrochloride and Fe^{2+} metal ions, which are positively charged on the surface of the adsorbent, the interaction between the hydroxyl group and the hydroxyl with metal ions is possible through the mechanism of formation of coordination complexes, chemical bonds that occur between active groups in organic molecules and metal ions can be explained by Lewis acid-base interactions that produce complexes on the solid surface, this phenomenon is due to metals having Lewis acid properties (Metiu et al., 2012), so the more metal cations added to activated charcoal, the greater the affinity for Lewis bases on tetracycline hydrochloride, for example hydroxyl groups, thereby increasing the adsorption.

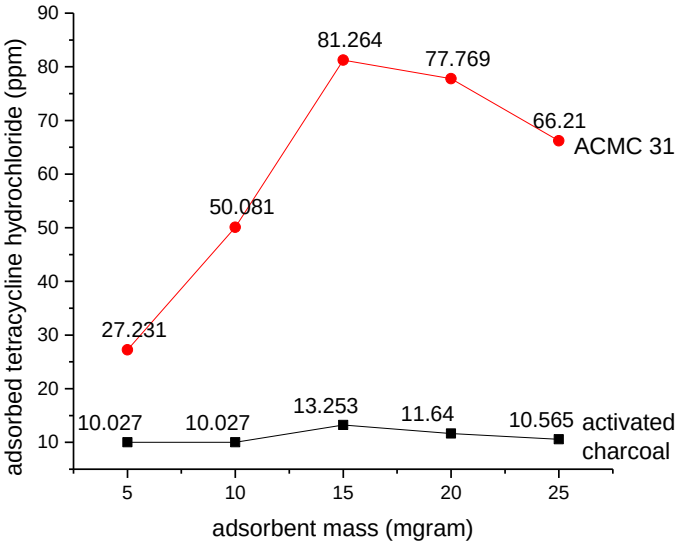

Figure 8. Results of tetracycline hydrochloride adsorption with variations in adsorbent mass

Difference Between Adsorbent Absorption and Contact Time

Contact time is required for activated charcoal and activated charcoal magnetic composites as adsorbents to interact with the adsorbate, namely tetracycline hydrochloride (**Figure 9**). At the beginning of the contact time, the adsorption takes place quickly because the active site on the adsorbent is still quite a lot, so that the frequency of bonding with the adsorbate molecule is quite high (Zian et al., 2016). The longer the contact time, the greater the interaction between the activated charcoal adsorbent and the magnetic composite of activated charcoal 3:1 with tetracycline hydrochloride. More and more tetracycline hydrochloride are adsorbed. The increase in the adsorption of the adsorbate was also caused by the fact that the adsorption equilibrium factor of the adsorbent to tetracycline hydrochloride had not been reached. The adsorption process will continue until all the active sides of the adsorbent are filled with an adsorbate. Adsorption continues until it reaches the optimum at a contact time of 60 minutes. When the adsorption equilibrium is reached, it is seen that the adsorption curve is no longer increasing but decreasing. At a contact time of more than 60 minutes, there was a decrease in the adsorption of tetracycline hydrochloride on the adsorbent because the adsorbent underwent a desorption process in this condition. The desorption process occurs because the adsorbate has saturated the surface of the adsorbent. Under these conditions, activated charcoal is unable to absorb more tetracycline hydrochloride. With increasing contact time, the amount of adsorbate adsorbed on the surface of the adsorbent increases until an equilibrium point is reached. The contact time between the adsorbent and the adsorbate that is too long can cause the adsorbent to become saturated and the adsorbate to be released (Zian et al., 2016).

Adsorption Kinetics

Adsorption kinetics (**Table 4**) is one of the important factors in the adsorption process because it shows the absorption rate of the adsorbent on the adsorbate and is influenced by contact time. The adsorption kinetics model of the tetracycline hydrochloride compound by ACMC 31 follows the Ho adsorption kinetics model. The kinetics model of Ho adsorption corresponds to pseudo-second-order with a constant adsorption rate of 0.0039 g/mg.min, which means 0.0039 g ACMC 31 can adsorb 1.0 mg of tetracycline hydrochloride in 1 minute. This means that the rate of adsorption of the tetracycline hydrochloride solution is influenced by the concentration of the adsorbate and the active site on the adsorbent.

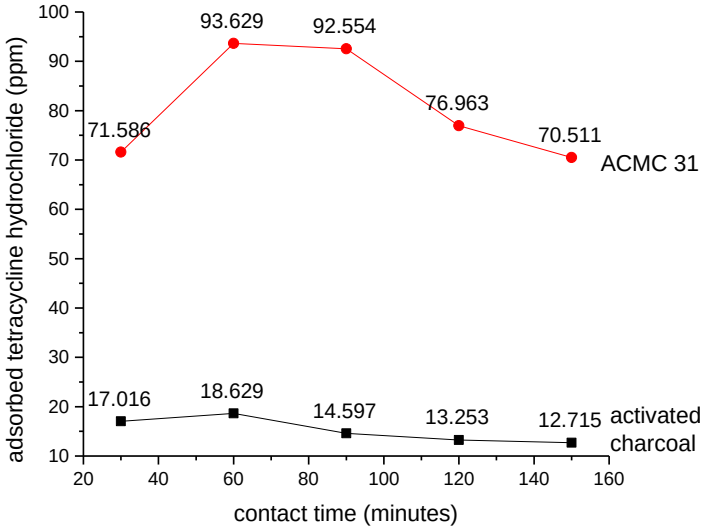

Figure 9. Results of tetracycline hydrochloride adsorption with variation of contact time

Table 4. Parameters of adsorption kinetics of Ho, Lagergreen, and Santosa of ACMC 31

Kinetics Model	Parameter	Value
Ho	R^2	0.9649
	K	0.0039 g/mg.min
	Qe	23.0947 mg/g
Lagergreen	R^2	0.0713
	K	0.0005 g/mg.min
	Qe	37.6262 mg/g
Santosa	R^2	0.0122
	K	0.0479 L/mol
	k	0.0004/min

Difference Between Adsorbent Absorption and Initial Adsorbate Concentration

Determination of the optimum concentration aims to determine the amount of the optimum adsorbate concentration that can be adsorbed by the adsorbent (**Figure 10**). The higher the concentration of adsorbate, the more concentration of tetracycline hydrochloride is adsorbed. However, under certain conditions, it will become stable because it has reached the saturation point so that an equilibrium process occurs. Inactivated charcoal magnetic composites with a concentration of tetracycline hydrochloride more than 100 ppm, there is a decrease in absorption efficiency because, at higher concentrations, the amount of tetracycline hydrochloride in solution is not proportional to the number of active sites on the available adsorbent so that the adsorbent surface will reach saturation point and the absorption efficiency also decreases.

Adsorption Isotherm

According to the adsorption mechanism, changes in the concentration of adsorbate by the adsorption process can be studied by determining the adsorption isotherm. The isotherm that shows the relationship between the concentration of tetracycline Hydrochloride absorbed (adsorbate) and the amount absorbed is the Langmuir and Freundlich adsorption isotherm. The Langmuir adsorption isotherm indicates that the adsorption process that occurs is a type of chemical adsorption, while the Freundlich adsorption isotherm indicates that the adsorption occurs physically.

The adsorption of tetracycline hydrochloride antibiotic solution using ACMC 31 followed the Freundlich isotherm model with a coefficient of determination (R^2) value of 0.7190 compared to the Langmuir isotherm model (**Table 5**). Thus, it can be assumed that the adsorbent surface is heterogeneous, and the adsorption forms many layers. This is because active adsorption sites have high affinity, and other parts have low affinity. However, the adsorbate is not strongly bound to the adsorbent. The adsorbate can move from one part of the adsorbent surface to another, and on the surface left by the adsorbate can be replaced by another. Activated charcoal magnetic composite has a heterogeneous surface shape because the surface pores of activated charcoal are surrounded and covered by small particles of $PbFe_2O_4$ magnetic composite. The Freundlich adsorption isotherm model also means that the adsorption process does not require heat to be uniformly or evenly distributed over the entire surface. When viewed from the value of 1/n, it can be concluded that the adsorption that occurs is favorable adsorption. This is because the value of 1/n is between 0 and 1, which is 0.4402, where if the value of 1/n is more than 1, then the adsorption that occurs is not profitable. Likewise, if the value of n = 1, then it can be interpreted that the process that occurs is irreversible, so there needs to be a drastic reduction in pressure or concentration to a lower value (Al-Ghouti & Da'ana, 2020).

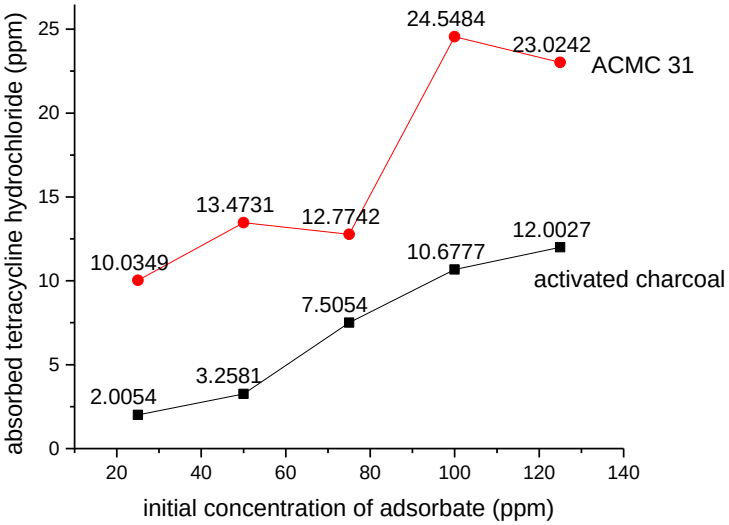

Figure 10. Results of tetracycline hydrochloride adsorption with variations in initial concentration

Table 5. Freundlich and Langmuir adsorption isotherms of ACMC31 adsorbent

Isotherms	Parameter	Value
Freundlich	R^2	0.7190
	K_f	180.1358 L/mg
	1/n	0.4402
Langmuir	R^2	0.6945
	K_L	0.049 L/mg
	q_m	76.3359 mg/g

The Langmuir equation determined the adsorption capacity of the tetracycline hydrochloride compound by ACMC 31 (**Table 5**). After calculating, the adsorption capacity of 76.3359 mg/g was obtained. The adsorption capacity of tetracycline hydrochloride by ACMC 31 is greater than other adsorbents, including Fe3O4@HCS (Yan et al., 2018), rice husk ash (Chen et al., 2016), Cu-immobilized alginate (Zhang et al., 2019), and iron-incorporated hydroxyapatite (Li et al., 2017). Although the adsorption capacity of ACMC 31 shows something good in absorbing tetracycline hydrochloride compounds, further modifications can still be made (for example, adding nanoparticles or using heating methods) to improve its performance as in the case of magnetic adsorbents carbon-coated cobalt oxide nanoparticles which have adsorption capacity reached 769.43 mg/g (Yang et al., 2020).

The Difference in the Absorption of the Adsorbent to the Acidity of the Adsorbate Solution

The pH value of the solution is one of the factors that affect the adsorption of tetracycline hydrochloride; with increasing pH, the proportion of negatively charged tetracycline hydrochloride molecules increases continuously. Tetracycline hydrochloride adsorption by activated charcoal is optimum at pH 8 and for adsorption using a magnetic composite of activated charcoal 3:1 optimum at pH 10 (**Figure 11**).

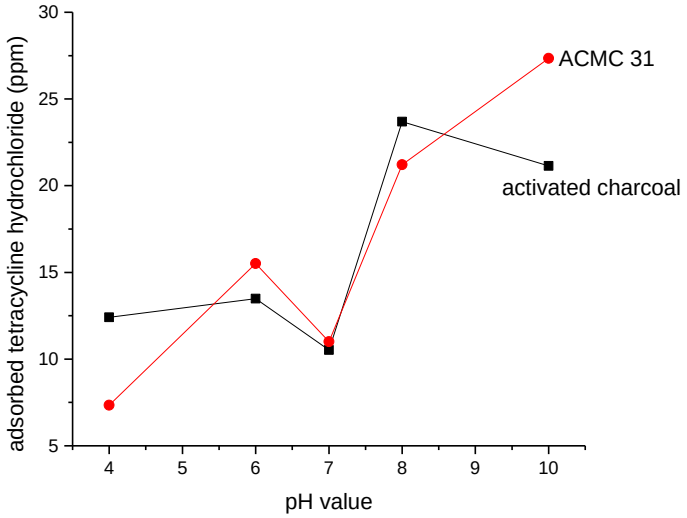

Figure 11. Results of tetracycline hydrochloride adsorption with variations in pH

Table 6. Adsorption of antibiotic using several adsorbents adsorbent

Types of antibiotics	Adsorben material	Adsorption capacity	Reference
Tetracycline hydrochloride	Rice hulk ash	8.37 mg/g	(Chen et al., 2016)
Ciprofloxacin	PAC@Fe3O4-MN	109.833 mg/g	(Al-Musawi et al., 2021)
Tetracycline hydrochloride	Sawdust activated charcoal	242.1308 mg/g	(Wardani et al., 2021)
Oxytetracycline hydrochloride	magnetic zeolite/Fe3O4 particles	83.33 mg/g	(Başkan et al., 2022)
Tetracycline	iron oxide	0.480	(K. Sun et al., 2022)
Amoxicillin	CTAB-activated Carbon from Peanut Husks	305 mg/g	(Egbedina et al., 2023)
Sulfadiazine	FO@CC-PM	214.07 mg.g	(M. Wang & You, 2023)
Ciprofloxacin	chitosan by TiO2@MWCNT nanohybrid	1510.5 mg/g	(Rostami et al., 2024)
Tetracycline hydrochloride	activated charcoal magnetic composites from Jengkol peels	76.3359 mg/g	This research

The pH value of the solution can greatly change the surface speciation of tetracycline hydrochloride. The effect of acidity on the adsorption of tetracycline hydrochloride is due to the interaction between the adsorbent and anionic TCH^- the concentration increases with increasing pH. TCH^- adsorption occurs because the anionic speciation of tetracycline hydrochloride interacts with the positive charge in activated charcoal and activated charcoal magnetic composites; this can increase TCH^- which is adsorbed at pH 10 by activated charcoal magnetic composites (Dehghan et al., 2018). Antibiotic adsorption can also

be carried out using other types of adsorbents as shown in **Table 6**.

CONCLUSIONS

In this study, activated charcoal material from the jengkol peel can be modified into an activated charcoal magnetic composite (ACMC). The magnetic properties present in ACMC are useful for facilitating the separation of the solution with the adsorbent in the separation process after adsorption. ACMC material has a greater absorption capacity than ordinary activated charcoal. The ACMC 31 material has a distinctly different structure from the other samples. Thus, the ACMC 31 material that has been made from jengkol peel waste can be potential as an antibiotic adsorbent, especially tetracycline hydrochloride compounds. This adsorbent can be an option to reduce antibiotic contamination in waters so that it can help in overcoming environmental problems.

ACKNOWLEDGMENTS

Our gratitude goes to the research and service center for the community of STIKes Bakti Tunas Husada Tasikmalaya, which has assisted in the form of research funds by research contract number 17a/i-SK/STIKes/XI/2020, so that this research can be completed properly.

REFERENCES

Akhtar, J., Amin, N. A. S., & Shahzad, K. (2016). A review on removal of pharmaceuticals from water by adsorption. *Desalination and Water Treatment*, *57*(27), 12842–12860. https://doi.org/10.1080/19443994.2015.1051121

Al-Ghouti, M. A., & Da'ana, D. A. (2020). Guidelines for the use and interpretation of adsorption isotherm models: A review. *Journal of Hazardous Materials*, *393*, 122383. https://doi.org/10.1016/j.jhazmat.2020.122383

Al-Musawi, T. J., Mahvi, A. H., Khatibi, A. D., & Balarak, D. (2021). Effective adsorption of ciprofloxacin antibiotic using powdered activated carbon magnetized by iron(III) oxide magnetic nanoparticles. *Journal of Porous Materials*, *28*(3), 835–852. https://doi.org/10.1007/s10934-021-01039-7

Azima, F., Nazir, N., & Sari, N. P. (2017). The making and characterization of Husk Jengkol's activated carbon as adsorbent. *International Journal on Advanced Science, Engineering and Information Technology*, *7*(3), 916–921. https://doi.org/10.18517/ijaseit.7.3.1084

Bakas, I., Elatmani, K., Qourzal, S., Barka, N., Assabbane, A., & Aît-Ichou, I. (2014). A comparative adsorption for the removal of p-cresol from aqueous solution onto granular activated charcoal and granular activated alumina. *Journal of Materials and Environmental Science*, *5*(3), 675–682.

Başkan, G., Açıkel, Ü., & Levent, M. (2022). Investigation of adsorption properties of oxytetracycline hydrochloride on magnetic zeolite/Fe_3O_4 particles. *Advanced Powder Technology*, *33*(6). https://doi.org/10.1016/j.apt.2022.103600

Bellusci, M., Albino, M., Masi, A., Peddis, D., Innocenti, C., & Varsano, F. (2024). High porosity-magnetic composite materials for magnetic induction swing adsorption (MISA): Improvement of performance properties. *Materials Chemistry and Physics*, *311*(October 2023), 128525. https://doi.org/10.1016/j.matchemphys.2023.128525

Bhatnagar, A., Hogland, W., Marques, M., & Sillanpää, M. (2013). An overview of the modification methods of activated carbon for its water treatment applications. *Chemical Engineering Journal*, *219*, 499–511. https://doi.org/10.1016/j.cej.2012.12.038

Chen, Y., Wang, F., Duan, L., Yang, H., & Gao, J. (2016). Tetracycline adsorption onto rice husk ash, an agricultural waste: Its kinetic and thermodynamic studies. *Journal of Molecular Liquids*, *222*, 487–494. https://doi.org/10.1016/j.molliq.2016.07.090

Conde-Cid, M., Fernández-Calviño, D., Nóvoa-Muñoz, J. C., Arias-Estévez, M., Díaz-Raviña, M., Fernández-Sanjurjo, M. J., Núñez-Delgado, A., & Álvarez-Rodríguez, E. (2018). Biotic and abiotic dissipation of tetracyclines using simulated sunlight and in the dark. *Science of the Total Environment*, *635*, 1520–1529. https://doi.org/10.1016/j.scitotenv.2018.04.233

Daghrir, R., & Drogui, P. (2013). Tetracycline antibiotics in the environment: A review. *Environmental Chemistry Letters*, *11*(3), 209–227. https://doi.org/10.1007/s10311-013-0404-8

Dehghan, A., Dehghani, M. H., Nabizadeh, R., Ramezanian, N., Alimohammadi, M., & Najafpoor, A. A. (2018). Adsorption and visible-light photocatalytic degradation of tetracycline hydrochloride from aqueous solutions using 3D hierarchical mesoporous BiOI: Synthesis and characterization, process optimization, adsorption and degradation modeling. In *Chemical Engineering Research and Design* (Vol. 129). Institution of Chemical Engineers. https://doi.org/10.1016/j.cherd.2017.11.003

Ding, C., He, J., Wu, H., & Zhang, X. (2021). Nanometer pore structure characterization of taiyuan formation shale in the lin-xing area based on nitrogen adsorption experiments. *Minerals*, *11*(3), 1–23. https://doi.org/10.3390/min11030298

Egbedina, A. O., Ugwuja, C. G., Dare, P. A., Sulaiman, H. D., Olu-Owolabi, B. I., & Adebowale, K. O. (2023). CTAB-activated carbon from peanut husks for the removal of antibiotics and antibiotic-resistant bacteria from water. *Environmental Processes*, *10*(2), 1–20. https://doi.org/10.1007/s40710-023-00636-9

Farzin Nejad, N., Shams, E., Amini, M. K., & Bennett, J. C. (2013). 239-246 Ordered mesoporous carbon CMK-5 as a potential sorbent for fuel desulfurization: Application to the removal of dibenzothiophene and comparison with CMK-3. *Microporous and Mesoporous Materials*, *168*, 239–246. https://doi.org/10.1016/j.micromeso.2012.10.012

Guo, Y., Huang, W., Chen, B., Zhao, Y., Liu, D., Sun, Y., & Gong, B. (2017). Removal of tetracycline from aqueous solution by MCM-41-zeolite a loaded nano zero valent iron: synthesis, characteristic, adsorption performance and mechanism. *Journal of Hazardous Materials*, *339*, 22–32. https://doi.org/10.1016/j.jhazmat.2017.06.006

Gusnidar, Yulnafatmawita, & Nofianti, R. (2011). Pengaruh kompos asal kulit jengkol (Phitecelobium jiringa (Jack) Prain ex King) terhadap ciri kimia tanah sawah dan produksi tanaman padi (The effect of compost from jengkol peel (Phitecelobium jiringa (Jack) Prain ex King) on the chemical characteristics of paddy soil and rice production). *Jurnal Solum*, *8*(2), 58–69. https://doi.org/10.25077/js.8.2.58-69.2011

Li, Y., Wang, S., Zhang, Y., Han, R., & Wei, W. (2017). Enhanced tetracycline adsorption onto hydroxyapatite by Fe(III) incorporation. *Journal of Molecular Liquids*, *247*, 171–181. https://doi.org/10.1016/j.molliq.2017.09.110

Lin, Z., Lin, N., Lin, H., & Zhang, W. (2020). Significance of PbO deposition ratio in activated carbon-based lead-carbon composites for lead-carbon battery under high-rate partial-state-of-charge operation. *Electrochimica Acta*, *338*, 135868. https://doi.org/10.1016/j.electacta.2020.135868

Liu, Y., Guo, L., Huang, H., Dou, J., Huang, Q., Gan, D., Chen, J., Li, Y., Zhang, X., & Wei, Y. (2019). Facile preparation of magnetic composites based on carbon nanotubes: Utilization for removal of environmental pollutants. *Journal of Colloid and Interface Science*, *545*, 8–15. https://doi.org/10.1016/j.jcis.2019.03.009

Liu, Y., Liu, X., Dong, W., Zhang, L., Kong, Q., & Wang, W. (2017). Efficient adsorption of sulfamethazine onto modified activated carbon: a plausible adsorption mechanism. *Scientific Reports*, *7*(1), 1–12. https://doi.org/10.1038/s41598-017-12805-6

Martins, A. C., Pezoti, O., Cazetta, A. L., Bedin, K. C., Yamazaki, D. A. S., Bandoch, G. F. G., Asefa, T., Visentainer, J. V., & Almeida, V. C. (2015). Removal of tetracycline by NaOH-activated carbon produced from macadamia nut shells: Kinetic and equilibrium studies. *Chemical Engineering Journal*, *260*, 291–299. https://doi.org/10.1016/j.cej.2014.09.017

Metiu, H., Chrétien, S., Hu, Z., Li, B., & Sun, X. (2012). Chemistry of Lewis acid-base pairs on oxide surfaces. *Journal of Physical Chemistry C*, *116*(19), 10439–10450. https://doi.org/10.1021/jp301341t

Nielsen, L., Biggs, M. J., Skinner, W., & Bandosz, T. J. (2014). The effects of activated carbon surface features on the reactive adsorption of carbamazepine and sulfamethoxazole. *Carbon*, *80*(1), 419–432. https://doi.org/10.1016/j.carbon.2014.08.081

Pérez-Ramírez, J., Christensen, C. H., Egeblad, K., Christensen, C. H., & Groen, J. C. (2008). Hierarchical zeolites: Enhanced utilisation of microporous crystals in catalysis by advances in materials design. *Chemical Society Reviews*, *37*(11), 2530–2542. https://doi.org/10.1039/b809030k

Rostami, M. S., Khodaei, M. M., & Benassi, E. (2024). Surface modified of chitosan by TiO_2@MWCNT nanohybrid for the efficient removal of organic dyes and antibiotics. *International Journal of Biological Macromolecules*, *274*(P1), 133382. https://doi.org/10.1016/j.ijbiomac.2024.133382

Shao, L., Ren, Z., Zhang, G., & Chen, L. (2012). Facile synthesis, characterization of a $MnFe_2O_4$/activated carbon magnetic composite and its effectiveness in tetracycline removal. *Materials Chemistry and Physics*, *135*, 16–24. https://doi.org/10.1016/j.matchemphys.2012.03.035

Shi, Y., Liu, G., Wang, L., & Zhang, H. (2019). Activated carbons derived from hydrothermal impregnation of sucrose with phosphoric acid: Remarkable adsorbents for sulfamethoxazole removal. *RSC Advances*, *9*(31), 17841–17851. https://doi.org/10.1039/c9ra02610j

Singh, R., Singh, A. P., Kumar, S., Giri, B. S., & Kim, K. H. (2019). Antibiotic resistance in major rivers in the world: A systematic review on occurrence, emergence, and management strategies. *Journal of Cleaner Production*, *234*, 1484–1505. https://doi.org/10.1016/j.jclepro.2019.06.243

Sivashankar, R., Sathya, A. B., Vasantharaj, K., & Sivasubramanian, V. (2014). Magnetic composite an environmental super adsorbent for dye sequestration - A review. *Environmental Nanotechnology, Monitoring and Management*, *1–2*, 36–49. https://doi.org/10.1016/j.enmm.2014.06.001

Smitha, P., Pandey, P. K., Kurian, S., & Gajbhiye, N. S. (2008). Mössbauer studies and magnetic properties of spinel lead ferrite. *Hyperfine Interactions*, *184*(1–3), 543–548. https://doi.org/10.1007/s10751-008-9777-7

Sun, K., Cheng, F., Liu, Y., Hua, Y., & Zhang, Y. (2022). Microwave-assisted iron oxide process for efficient removal of tetracycline. *Journal of Environmental Management*, *307*(December 2021), 114600. https://doi.org/10.1016/j.jenvman.2022.114600

Sun, M. H., Huang, S. Z., Chen, L. H., Li, Y., Yang, X. Y., Yuan, Z. Y., & Su, B. L. (2016). Applications of hierarchically structured porous materials from energy storage and conversion, catalysis, photocatalysis, adsorption, separation, and sensing to biomedicine. *Chemical Society Reviews*, *45*(12), 3479–3563. https://doi.org/10.1039/c6cs00135a

Wang, M., & You, X. yi. (2023). Efficient adsorption of antibiotics and heavy metals from aqueous solution by structural designed PSSMA-functionalized-chitosan magnetic composite. *Chemical Engineering Journal*, *454*(November 2022). https://doi.org/10.1016/j.cej.2022.140417

Wang, Q., Duan, Y. J., Wang, S. P., Wang, L. T., Hou, Z. L., Cui, Y. X., Hou, J., Das, R., Mao, D. Q., & Luo, Y. (2020). Occurrence and distribution of clinical and veterinary antibiotics in the faeces of a Chinese population. *Journal of Hazardous Materials*, *383*(August 2019), 121129. https://doi.org/10.1016/j.jhazmat.2019.121129

Wang, Y. X., Chou, S. L., Kim, J. H., Liu, H. K., & Dou, S. X. (2013). Nanocomposites of silicon and carbon derived from coal tar pitch: Cheap anode materials for lithium-ion batteries with long cycle life and enhanced capacity. *Electrochimica Acta*, *93*, 213–221. https://doi.org/10.1016/j.electacta.2013.01.092

Wardani, G. A., Qudsi, E. M., Pratita, A. T. K., Idacahyati, K., & Nofiyanti, E. (2021). Utilization of activated charcoal from sawdust as an antibiotic adsorbent of tetracycline hydrochloride. *Science and Technology Indonesia*, *6*(3), 181–188. https://doi.org/10.26554/sti.2021.6.3.181-188

Yan, X., Gan, K., Tian, B., Zhang, J., Wang, L., & Lu, D. (2018). Photo-fenton refreshable Fe_3O_4@HCS adsorbent for the elimination of tetracycline hydrochloride. *Research on Chemical Intermediates*, *44*(1). https://doi.org/10.1007/s11164-017-3028-y

Yang, G., Gao, Q., Yang, S., Yin, S., Cai, X., Yu, X., Zhang, S., & Fang, Y. (2020). Strong adsorption of tetracycline hydrochloride on magnetic carbon-coated cobalt oxide nanoparticles. *Chemosphere*, *239*(January), 124831. https://doi.org/10.1016/j.chemosphere.2019.124831

Zhang, Xiaonuo, Lin, X., He, Y., Chen, Y., Luo, X., & Shang, R. (2019). Study on adsorption of tetracycline by Cu-immobilized alginate adsorbent from water environment. *International Journal of Biological Macromolecules*, *124*, 418–428. https://doi.org/10.1016/j.ijbiomac.2018.11.218

Zhang, Xueyang, Gao, B., Creamer, A. E., Cao, C., & Li, Y. (2017). Adsorption of VOCs onto engineered carbon materials: A review. *Journal of Hazardous Materials*, *338*, 102–123. https://doi.org/10.1016/j.jhazmat.2017.05.013

Zian, Ulfin, I., & Harmami. (2016). Pegaruh waktu kontak pada adsorpsi Remazol Violet 5R menggunakan adsorben Nata de Coco (Effect of contact time on the adsorption of Remazol Violet 5R using Nata de Coco adsorbent). *Jurnal Sains Dan Seni ITS*, *5*(2), 107–110.